Operational Planning and Optimisation in Active Distribution Networks using Modern Intelligent Power Flow Controllers

Operational Planning and Optimisation in Active Distribution Networks using Modern Intelligent Power Flow Controllers

Ahmad Asrul Ibrahim
School of Engineering and Computing
Sciences
Durham University
Durham, United Kingdom
a.a.ibrahim@durham.ac.uk

Behzad Kazemtabrizi
School of Engineering and Computing
Sciences
Durham University
Durham, United Kingdom
behzad.kazemtabrizi@durham.ac.uk

Chris Dent
School of Engineering and Computing
Sciences
Durham University
Durham, United Kingdom
chris.dent@durham.ac.uk

Abstract—**In this paper, a centralised control framework is introduced for day-ahead operational planning of active distribution networks which accommodate high levels of distributed generation resources. The purpose of the framework is to plan network operation in order to minimise power curtailment from distributed generation and maintaining acceptable levels of voltage regulation throughout the network. For this purpose, both power flow control and rapid network reconfiguration have been considered as various acceptable levels of control available to the network operator to provide required levels of operational flexibility. The power flow control within the network is promised by the application of fully controlled back-back voltage source converters placed in key points (both normally-open and normally-close) in the network. Meanwhile, the network reconfiguration constraints guarantee that radial topology is always maintained in order to avoid tremendous changes in the protection system coordination. The operation of a modified 33-bus system exemplar is analysed in three case studies namely, passive network (base case), active network using remote-controlled switches and active network using intelligent power converters. Results show a significant saving in terms of operational costs as well as transmission losses in *active* cases despite the radial constraint condition in place.**

Index Terms -- **Active distribution system, back-to-back voltage source converters, network reconfiguration, optimal power flow, voltage constraints management**

I. INTRODUCTION

Most countries have now adopted a greener energy generation portfolio which mostly is based on using renewable energy resources. A large capacity of renewable energy generation comes in form of small-scale distributed generations (DGs) which are integrated in distribution (medium and low voltage) networks [1]. However, the low ratio of reactance-to-resistance in radial MV/LV networks implies a higher sensitivity of voltage fluctuations to active power injections from variable DG resources [1]. In order to avoid voltage problems, in an active distribution system (ADS), DG outputs are controlled in a manner set by network operators which imposes DG power curtailment when

necessary [2]. Consequently, several voltage constraints management schemes have been proposed to reduce DG power curtailment. The schemes include coordinated Volt-Var control [3], coordinated dispatch of distributed energy resources [4], and reactive power compensators (e.g. shunt capacitor, static Var compensator) [5]. Recently, network reconfiguration has attracted research interest in the field especially with rising penetration levels of DG in distribution networks [6-9]. The approaches are applied to achieve certain objectives including, but not limited to, loss minimisation [6], reliability improvement [7], grid supply reduction [8] and DG power curtailment minimisation [9]. Network reconfiguration is applied by altering the structure of the network topology via changing status of sectionalising (normally-close) and tie switches (normally-open) in the system. In order to facilitate coordination of over-current protection relays, it is preferred that network topology stays radial at all times within network reconfiguration scheme. By doing this, power flow from generation to demand can be re-routed through less sensitive feeders to improve the system voltage profile [6]. However, intermittent behaviour of demand and DG supplies causes rapid change of the switches operation to manage voltage fluctuations [9]. Thus, online application of the network reconfiguration would shorten the switches' lifetime.

Power electronic devices are a good alternative to the conventional remote-controlled switches for a variety of network applications including network reconfiguration. In [10-12], a back-to-back (BTB) arrangement of voltage source converters (VSCs) are suggested to be installed at normally-open points between adjacent feeders for creating loops between feeders. This topology is normally known as a Soft Normally Open Point (SNOP). The main advantage of using BTB-VSCs over the conventional remote-controlled switches (RCSs) is that it provides active and reactive power flow control at its interface terminals, thus improving the reliability and stability of the operation of the network [10]. However, such studies typically do not consider suitable operational constraints to avoid undesired misconfiguration in the existing protection coordination schemes. The easiest way to address

this issue at low investment on the protection coordination is by introducing a set of suitable operational constraints that would maintain the network's radial topology [13]. Since the BTB-VSC is used to control power flows at its interface terminals, it clearly has capability of blocking power flows which means it can act as a controlled switch. In this paper, the concept of SNOPs previously introduced in [10-12] has been generalised to applications in both normally open and close points for both network reconfiguration and power flow control purposes.

The contributions of this paper are therefore three-fold: (i) the centralised management framework in [9] has been extended to include control settings of BTB-VSCs for a day-ahead operational network planning, (ii) to ensure a realistic power flow control operation, a generalised explicit model for the BTB-VSCs is introduced which incorporates the converters realistic operational limits, and (iii) to ensure enforcement of a radial topology, a binary decision variable within the BTB-VSC operational constraints is introduced to efficiently exploit the existing radial topology requirement. Studying on radial topology makes this work differ from [11] and inappropriate to be compared.

This paper is organized as follows: Section II describes the derivation of the generalised BTB-VSC model that explicitly addresses radial configuration constraints. Section III presents a multi-period optimal power flow formulation for implementation of the centralised control framework. Section IV highlights the difference in explicit control variables between RCSs and BTB-VSCs. Section V discusses on the three distinct case studies investigated in this work and followed by conclusions in section VI.

II. GENERALISED BTB-VSC POWER-LINE MODEL

A. Voltage Source Converter (VSC) Full Model

The basic 3-phase full bridge voltage source converter shown in Fig (1a) forms the essence of the mathematical model presented here which is an extension of the model presented in [14-15]. It has been observed that for purposes of efficient computational modelling the converter could be represented as essentially an ideal transformer with complex tap ($\bar{m}_a = m_a e^{j\phi}$) whose magnitude corresponds to the actual PWM amplitude modulation ratio and phase shift corresponds to the actual phase shift, relative to system reference, that can be exerted at the output AC voltage (RMS, line-line). For an actual VSC with a DC input voltage of E_{dc} the AC output voltage at converter terminals then becomes:

$$\bar{V}_{cr} = k\bar{m}_a E_{dc} \qquad (1)$$

For a two-level converter k ≈ 0.612 and this model can be extended for any type of converter at any switching level [15]. The advantage of this model is that it combines both DC and AC sides on one single frame of reference for efficient load flow calculations. It also does not neglect the operational limits imposed on the converter for linear operation (i.e. $0 \leq m_a \leq 1$) [15]. The converter in the linear region is then able to provide independent active and reactive power through controlling its AC output terminal voltage. Furthermore,

using the *ideal transformer* model, a realistic operational capability curve for the VSC may also be derived which is shown in Fig (1b) which takes into account the limiting factors of the VSC operation, namely the switching devices (i.e., IGBTs) current limit, the DC bus voltage, E_{dc}, and the DC cable current limit [16].

a) An equivalent VSC model   b) Limitation factors of VSC operation
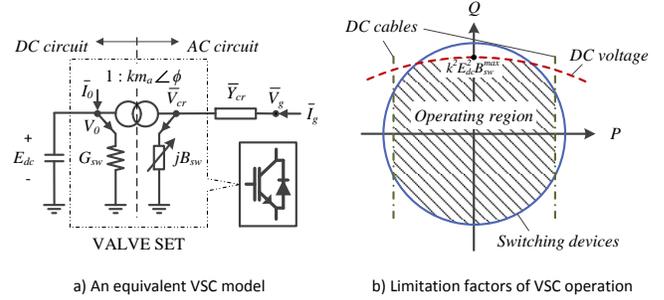
Figure 1.   An equivalent VSC model and its operation capability

Note that the shunt branch, B_{sw} in Fig (1a) is used to impose a zero reactive power flow constraint on the DC circuit. This notional susceptance thus models the leading or lagging VAR operation through PWM switching action in the converter. Other elements of the circuit are the interface admittance, $\bar{Y}_{cr}$ and the shunt resistor (conductance, G_{sw}) to represent switching power loss of the VSC for a given PWM switching frequency. Accordingly, the nodal current injections can be expressed as [14-15]:

$$\underbrace{\begin{pmatrix} \bar{I}_g \\ \bar{I}_0 \end{pmatrix}}_{\bar{I}} = \underbrace{\begin{pmatrix} \bar{Y}_{cr} & -km_a\bar{Y}_{cr}e^{j\phi} \\ -km_a\bar{Y}_{cr}e^{-j\phi} & G_{sw}+k^2m_a^2(\bar{Y}_{cr}+jB_{sw}) \end{pmatrix}}_{\bar{Y}_{[2\times2]}} \underbrace{\begin{pmatrix} \bar{V}_g \\ E_{dc} \end{pmatrix}}_{\bar{V}} \qquad (2)$$

The nodal power injections $\bar{S} = (\bar{S}_g, \bar{S}_0)^T$ can then be calculated as below:

$$\bar{S} = diag(\bar{V})\cdot\bar{I}^* = diag(\bar{V})\{\bar{Y}_{[2\times2]}^*\cdot\bar{V}^*\} \qquad (3)$$

B. BTB-VSC Nodal Powers

Fig (2) shows the BTB-VSC connected to an adjacent medium voltage line via a phase reactor, x_{cr}, for power flow control purposes.
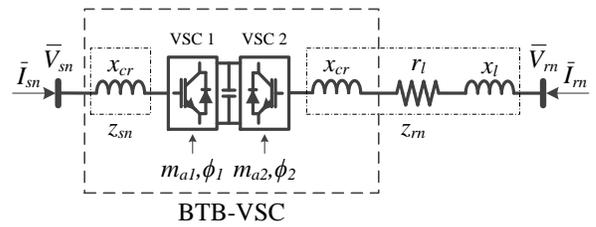
Figure 2.   An equivalent power line with a connected BTB-VSC

Knowing (3) the nodal powers at the sending (*sn*) and receiving ends *(rn)* of the BTB-VSC power line can be derived as follows:

$$\bar{S}_{sn} = P_{sn} + jQ_{sn} = \bar{Y}_{sn}^*V_{sn}^2 - km_{a1}e^{-j\phi_1}\bar{Y}_{sn}^*E_{dc}\bar{V}_{sn} \qquad (4)$$

$$\bar{S}_{rn} = P_{rn} + jQ_{rn} = \bar{Y}_{rn}^*V_{rn}^2 - km_{a2}e^{-j\phi_2}\bar{Y}_{rn}^*E_{dc}\bar{V}_{rn} \qquad (5)$$

In (4) and (5), the equivalent admittance values are:

$$\overline{Y}_{sn} = -j/x_{cr} \tag{6}$$

$$\overline{Y}_m = \frac{r_l - j(x_{cr} + x_l)}{r_l^2 + (x_{cr} + x_l)^2} \tag{7}$$

As can be seen in Fig (2) that both converters (VSC 1 and 2) are connected at a common DC bus, the following power balance constraint, which is derived from DC side of power injections in (3), must be fulfilled:

$$\overline{S}_{01} + \overline{S}_{02} = 0 \tag{8}$$

$$\overline{S}_{01} = P_{01} + jQ_{01} = G_{sw1}E_{dc}^2 + (\overline{Y}_{sn}^* - jB_{sw1})k^2 m_{a1}^2 E_{dc}^2 - km_{a1}e^{j\phi_1}\overline{Y}_{sn}^* E_{dc}\overline{V}_{sn}^* \tag{9}$$

$$\overline{S}_{02} = P_{02} + jQ_{02} = G_{sw2}E_{dc}^2 + (\overline{Y}_m^* - jB_{sw2})k^2 m_{a2}^2 E_{dc}^2 - km_{a2}e^{j\phi_2}\overline{Y}_m^* E_{dc}\overline{V}_m^* \tag{10}$$

In this study, it is assumed that the switching loss of the VSCs is negligible ($G_{sw1} = G_{sw2} \approx 0$). As discussed earlier, the reactive power injections in DC circuit are kept at zero by imposing an appropriate constraint ($Q_{01}=Q_{02}=0$). The values of B_{sw1} and B_{sw2} correspond to converter reactive power output as function of modulation ratio and phase angle. That means each converter controls reactive power independently which are given by B_{sw1} and B_{sw2}, respectively.

C. Radiality Constraint

In order to maintain network radial topology, this model requires binary decision variables, s_c to enforce zero power flow constraint at the controlled lines when it is needed for network reconfiguration purposes. This will be added into BTB-VSC operation limits that will be explained in the next sub-section. Radial structure of the network can be obtained by ensuring the number of blocked lines (zero power flow) must be exchanged with the same number of other controlled lines (installed with BTB-VSC) [9] as:

$$\sum_{c \in C} s_c = \sum_{c \in C} s_c^0 \tag{11}$$

where, C is the subset of lines with BTB-VSC and s_c^0 is the initial status of controlled lines in a radial distribution network. However, this constraint alone is insufficient and might cause zero-injection at some buses [17]. In order to overcome this problem, all possible paths to link between region R and the grid supply point (GSP) are identified, $\Pi^R = \left\{ \pi_1^R, \pi_2^R, \ldots, \pi_k^R \right\}$ in which π_k^R is 1 in case of an active k-th path and zero otherwise. Each region must have at least one active path to the GSP using the following constraint:

$$\sum_{\pi_k^R \in \Pi^R} \pi_k^R(s_c) \geq 1 \ , \ \forall R \tag{12}$$

D. Converter Operating Limits

As mentioned earlier, VSC operation is also restricted by current limit of the switching devices (IGBTs) and DC cables. Assume that BTB-VSC is designed with higher current rating of DC cables; the limits can be addressed solely using IGBT's current rating. Therefore, the AC current injections of both VSCs (VSC 1 and 2) must fulfill the following constraints, derived from (4) and (5), respectively:

$$Y_{sn}^2[V_{sn}^2 + k^2 m_{a1}^2 E_{dc}^2 - 2km_{a1}E_{dc}V_{sn}\cos(\theta_{sn} - \phi_1)] \leq I_{rate}^2 \tag{13}$$

$$Y_m^2[V_m^2 + k^2 m_{a2}^2 E_{dc}^2 - 2km_{a2}E_{dc}V_m\cos(\theta_m - \phi_2)] \leq s_c I_{rate}^2 \tag{14}$$

where, I_{rate} is the current limit of VSC. A binary variable, s_c as discussed earlier is used to suppress the current flow through the controlled lines when it is necessary to enforce radiality.

III. MULTI-PERIOD OPF FORMULATION

The centralised control framework proposed in this paper uses multi-period optimal power flow (OPF) for near-real-time (day-ahead) operational planning of the medium voltage distribution network. The demand and DG generation outputs are forecast for the day-ahead and are fed to an OPF solver in the central controller. The multi-period OPF formulation within the central controller framework in more detail is given in Appendix A. Overall control framework operation is shown graphically in the flow chart of Fig (3). In this figure, x is the vector of state variables and u is the vector of control variables associated with the DGs, OLTC and BTB-VSCs settings. For comparison purposes, control variables for RCSs are used to replace BTB-VSCs as introduced in next section.
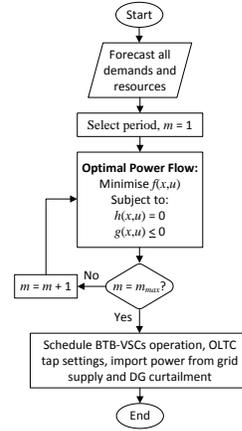
Figure 3. A flowchart of multi-period OPF in the control framework

IV. EXPLICIT CONTROL VARIABLES

It is necessary to explicitly define the control variables associated with the RCS as presented in [9] and BTB-VSCs which are used to formulate the OPF problem in this paper for the central control framework. All variables are kept within their respective limits.

A. Remote-controlled switches (RCSs)

In the traditional network reconfiguration, few lines are selected to install with RCS so that power flow in the network can be managed via re-routing procedure. The procedure is carried out by changing the status of the switches (i.e. open or close) either to allow current to flow through the lines or not. When the switch is closed, active and reactive power flow at the defined line will be totally corresponded to the system operation without any other control capability.

B. BTB-VSCs

As discussed in section II, each VSC uses *three* explicit control variables; modulation index and phase angle as well as the variable shunt susceptance corresponding to converter VAR operation. The binary variable, s_c introduced in section II.C is used to enforce radiality constraint for network

reconfiguration. As expressed in (14), power flow through the controlled lines can be blocked by enforcing a zero current injection constraint through the application of the binary variable, s_c. In actuality this produces a set of AC voltage magnitude and angle at the converter's terminal, as shown in (1), matching the system voltage phasor. Moreover, BTB-VSC can provide reactive power control regardless of the state of the lines to which they are connected. If C is the set of all BTB-VSCs, then the control variables are defined as:

$$u_{BTB-VSC} = (m_{a\{c\}}, \phi_c, B_{sw\{c\}}, s_c) \quad \forall c \in C \quad (15)$$

V. CASE STUDIES AND RESULTS

This optimisation problem has been formulated in AIMMS modelling environment [18]. The problem is solved using KNITRO 9.0 on a PC of 3.5 GHz and 8 GB RAM. It also has been formulated in AMPL language [19] and solved using mixed integer nonlinear programming (MINLP) algorithm developed by Roger Fletcher and Sven Lyeffer within NEOS Server [20] for validating purposes. Both KNITRO 9.0 in AIMMS and MINLP in NEOS Server are converged to the same solution in all cases. The average computational time by KNITRO 9.0 in AIMMS is 64 seconds.

A. Test network

The proposed framework is applied on a modified of 33-bus benchmark test network in [21] as shown in Fig (4). We assume voltage limits of 0.95/1.05 p.u. at all buses and thermal limit of lines, S_{max} = 5 MVA. An active distribution system actively manages all control devices in the network within their operation settings as given in Appendix B.
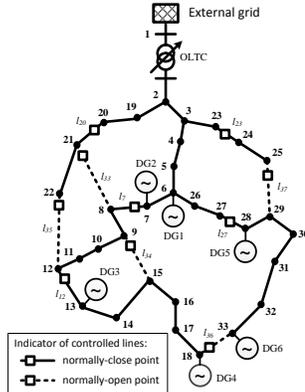
Figure 4. A modified 33-bus test system

Three different scenarios are considered namely, a normal operation (day-ahead scheduling) and two worst case scenarios (high demand/ no generation and low demand/ high generation) for each case study mentioned in Table I. The results are analysed in terms of system losses, DG curtailment, tap changer operation, line loadings, control settings for BTB-VSCs and the subsequent operation cost.

TABLE I: CASE STUDIES

Case	P control	Q control	State of network	Network reconfiguration
Base case	N/A	N/A	Passive	No
RCSs	N/A	N/A	Active	Yes (RCS)
BTB-VSCs	Yes	Yes	Active	Yes (BTB-VSC)

B. Daily operational planning

The proposed framework can be applied for optimum day-ahead operational planning of network controllers where demand and DG output are normally available from forecast data. In this case study, forecast data of daily demand and generation are assumed as in Table V in Appendix B to obtain network configuration in each time period, m within a 24-hour window. Table II shows the summary of network operation for three cases with the objective of minimising DG curtailment and power losses at the same time. The objective function is given in Appendix A. The total energy of 43.2 kWh from renewable resources could be fully utilised when network reconfiguration is applied. It is also apparent that when it comes to energy losses the proposed approach using BTB-VSCs gives a much better performance than RCSs. As a result, less dependency to the external grid could be achieved. Ultimately, the proposed approach indicates a significant total cost reduction in terms of DG curtailment and power losses up to 80.7% for daily operation.

TABLE II: PERFORMANCE OF DIFFERENT APPROACHES IN DAILY OPERATION

Item	NR Approach		
	Base Case	RCSs [9]	BTB-VSCs
Energy losses (kWh)	2561	1670	1086
Energy curtailed (kWh)	43.2	0	0
Net energy import (kWh)	29934.5	28934.0	28350.2
Total operation cost ($)	8.04	2.69	1.55
Total cost reduction	-	66.5%	**80.7%**

Fig (5a) shows obtained voltage profile at bus 18 (as one of the nodes of interest) for all three test cases. Referring to the base case, voltage magnitudes at some buses (particularly bus 18) are violating the upper limit due to high injection of power from DGs in which requires some amount of energy to be curtailed. Instead, the voltage constraints can be managed without curtailment via either using RCSs or BTB-VSCs. Results clearly show that BTB-VSCs are a better option to RCSs. In this case using BTB-VSCs can reduce line losses significantly by maintaining the nodal voltage at bus 18 close to its upper limit. This is made possible through reactive power injection of the VSC adjacent to bus 18. The optimal daily operation settings of the VSC (modulation index, phase angle and VAR operation) are presented in Fig (5b) and (5c).
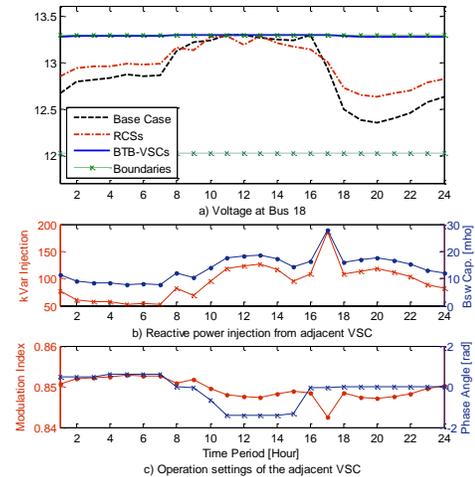
Figure 5. Voltage magnitude at bus 18 and adjacent VSC operation

Furthermore, analysis on loading factors of the relevant equipment for three case studies is carried out to highlight the benefits of using BTB-VSCs. Fig (6a) illustrates the highest line loading at each time period for all three cases. Network reconfiguration using RCSs provides almost same loading with base case except when DG output is higher than demand (hour 9 and 15). On the other hand, a significant line loading improvement can be seen at each time period when BTB-VSCs are used. OLTC burden, indicated by changes of tap position, in daily operation is also compared between different cases as depicted in Fig (6b). Tap position is varying 8 steps in base case which is reduced to 5 steps using RCSs and further reduced to 2 steps using BTB-VSCs approach.
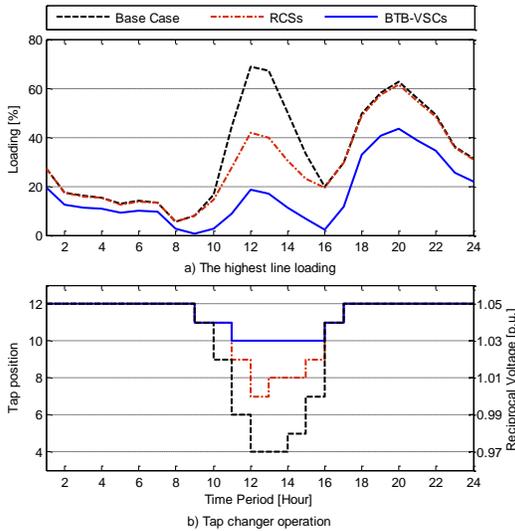
Figure 6. Daily performance on line loading and tap operation

This experimental result suggested that RCSs has changed the status of line at least twice a day. In other words, annual operation requires at least 730 times (365 days × 2 times/day) for this application. Thus, the approach based on RCSs is impractical as it will shorten the switch's lifetime due to rapid changes of the switch status.

C. Worst-case scenarios tests

In addition to daily operation, two worst-case scenarios have also been presented, namely; a) high demand during periods of no generation, b) low demand during periods of high generation. Although the scenarios rarely occur in reality, they are worth investigating as their outcomes are potentially severe. The performance comparison is presented in Table III. It is clearly shown that BTB-VSCs could reduce burden on the OLTC operation. The highest line loading is significantly improved using BTB-VSCs for a situation of high demand/no generation. At low demand/high generation, line loading might be violated if DG curtailment is not available in the base case. Therefore, higher line loading is observed using RCSs as to accommodate more power generation from DGs. Instead, replacing RCSs with BTB-VSCs will result in improved line loadings without any DG curtailment. Furthermore, the overall system loss is significantly improved in both scenarios when using BTB-VSCs. Overall, BTB-VSCs approach has showed the best performance as indicated by its operation cost.

TABLE III: A Performance Comparison of Worst-Case Scenarios

Item	High demand – no generation			Low demand – high generation		
	Base Case	RCSs [9]	BTB-VSCs	Base Case	RCSs [9]	BTB-VSCs
Tap position	12	12	12	3	4	9
Highest line loading	77%	75%	53%	72%	83%	71%
Power losses (kW)	181	138	99	306	250	222
Power curtailed (kW)				910	0	0
Operation cost ($/h)	0.58	0.28	0.17	23.69	0.66	0.55

VI. Conclusion

This paper proposes a new control framework for operational planning in active distribution networks using BTB-VSCs for purposes of flexible power flow control and network reconfiguration with additional network radiality constraints imposed. A multi-period OPF formulation is applied on the modified 33-bus test network to showcase the performance of the proposed framework, in terms of savings in total operational costs, when compared to traditional network reconfiguration approaches using conventional RCSs. The results show that using BTB-VSCs instead of RCSs acting as both normally open and normally close switches for fast network reconfiguration would lead to far superior operational flexibility, which could ultimately reduce overall operational burden on network devices such as the OLTC as well as a reduction in line loading. Moreover, as BTB-VSCs are static devices they are subject to less levels of mechanical stress when subject to a continuously varying operational regime. The results presented in this paper also show that operational flexibility promised by BTB-VSCs will reduce the DG curtailment and would be beneficial from an economic perspective encouraging toward more renewable DG resources at medium voltage levels.

References

[1] T.C. Green, R.W. Silversides and T. Lüth, "Power electronics in distribution system management," *HubNet Position Paper*, 2015.

[2] Q. Zhou and J. Bialek, "Generation curtailment to manage voltage constraints in distribution networks," *IET Generation, Transmission & Distribution*, vol. 1, pp. 492–498, 2007.

[3] S. Auchariyamet and S. Sirisumrannukul, "Optimal daily coordination of Volt/VAR control devices in distribution systems with distributed generators," in Proc. *45th International Universities Power Engineering Conference (UPEC)*, Cardiff, Wales, pp. 1-6, 2010.

[4] G. Carpinelli, G. Celli, S. Mocci, F. Mottola, F. Pilo and D. Proto, "Optimal integration of distributed energy storage devices in smart grids," *IEEE Transactions on Smart Grid*, vol. 4, no. 2, pp. 985–995, 2013.

[5] J. Lakkireddy, R. Rastgoufard, I. Leevongwat and P. Rastgoufard, "Steady state voltage stability enhancement using shunt and series FACTS devices," in Proc. *Power Systems Conference (PSC)*, Clemson University, USA, pp.1-5, 2015.

[6] S. Naveen, K.S. Kumar and K. Rajalakshmi, "Distribution system reconfiguration for loss minimization using modified bacterial foraging optimization algorithm," *Electrical Power and Energy Systems*, vol. 69, pp. 90–97, 2015.

[7] C. Lee, C. Liu, S. Mehrotra and Z. Bie, "Robust Distribution Network Reconfiguration," *IEEE Transactions on Smart Grid*, vol. 6, no. 2, pp. 836–842, 2015.

[8] Q. Peng, Y. Tang and S.H. Low, "Feeder Reconfiguration in Distribution Networks Based on Convex Relaxation of OPF," *IEEE Transactions on Power Systems*, vol. 30, no. 4, pp. 1793–1804, 2015.

[9] F. Capitanescu, L.F. Ochoa, H. Margossian and N.D. Hatziargyriou, "Assessing the potential of network reconfiguration to improve

distributed generation hosting capacity in active distribution systems," *IEEE Transactions on Power Systems*, vol. 30, no. 1, pp. 346–356, 2015.

[10] J.M. Bloemink and T.C. Green, "Increasing photovoltaic penetration with local energy storage and soft normally-open points," in Proc. *2011 IEEE Power and Energy Society General Meeting*, San Diego, California, pp. 1-8, 2011.

[11] W. Cao, J. Wu and N. Jenkins, "Feeder load balancing in MV distribution networks using soft normally-open points," in Proc. *5th IEEE PES Innovative Smart Grid Technologies Europe (ISGT)*, Istanbul, Turkey, pp. 1-8, 2014.

[12] J.M. Bloemink and T.C. Green, "Benefits of distribution-level power electronics for supporting distributed generation growth," *IEEE Transactions on Power Delivery*, vol. 28, no. 2, pp. 911–919, 2013.

[13] S.A.M. Javadian, R. Tamizkar and M.R. Haghifam, "A protection and reconfiguration scheme for distribution networks with DG," in Proc. *2009 IEEE Bucharest Power Tech Conference*, Bucharest, Romania, pp. 1-8, 2009.

[14] E. Acha, B. Kazemtabrizi and L.M. Castro, "A New VSC-HVDC Model for Power Flows Using the Newton-Raphson Method," *IEEE Transactions on Power Systems*, vol. 28, no. 3, pp. 2602–2612, 2013.

[15] B. Kazemtabrizi and E. Acha, "An Advanced STATCOM Model for Optimal Power Flows Using Newton's Method," *IEEE Transactions on Power Systems*, vol. 29, no. 2, pp. 514–525, 2014.

[16] S.G. Johansson, G. Asplund, E. Jansson and R. Rudervall, "Power system stability benefits with VSC DC-transmission systems," in Proc. CIGRE 2004 Session, Paris, France, 2004.

[17] E.R. Ramos, J.R. Santos and J. Reyes, "A simpler and exact mathematical model for the computation of the minimal power losses tree," *Electric Power System Research*, vol. 80, no. 5, pp. 562–571, 2010.

[18] J. Bisschop and M. Roelofs. *AIMMS Language Reference, Version 3.12*. Haarlem, Netherlands: Paragon Decision Technology, 2011.

[19] R. Fourer, D.M. Gay and B.W. Kernighan. *AMPL – A Mathematical Programming Language*. Thomson, Second Ed., 2003.

[20] J. Czyzyk, M.P. Mesnier and J.J. More. The Network-Enabled Optimization System (NEOS) Server. Argonne National Laboratory: Argone, Illinois, 1997.

[21] M. E. Baran and F. F. Wu, "Network reconfiguration in distribution systems for loss reduction and load balancing," *IEEE Transactions on Power Delivery*, vol. 4, no. 2, pp. 1401–1497, 1989.

APPENDIX A:
FULL OPF FORMULATION

Let *N, G, E, L, T, C,* and *M* denote the sets of respectively, nodes, DGs, grid supply points (GSP), power lines, the subset of lines with on-load tap changer (OLTC) transformers, the subset of lines with BTB-VSCs, and time periods. The full optimal operation planning in period $m \in M$ is formulated as a full AC optimal power flow problem as below:

$$\min\left\{\sum_{m\in M}\sum_{g\in G}[c_1(P_{ava\{g\}}^m - P_g^m)^2 + c_2(P_{ava\{g\}}^m - P_g^m)]\right.$$

$$\left. + \sum_{m\in M}\sum_{l\in L}[c_1(P_{sn\{l\}}^m + P_{m\{l\}}^m)^2 + c_2(P_{sn\{l\}}^m + P_{m\{l\}}^m)]\right\}$$ (16)

$$P_e^{\min} \le P_e^m \le P_e^{\max} \qquad \forall e \in E \quad (17)$$

$$Q_e^{\min} \le Q_e^m \le Q_e^{\max} \qquad \forall e \in E \quad (18)$$

$$0 \le P_g^m \le P_{ava}^m \qquad \forall g \in G \quad (19)$$

$$tp_o^m \in \{tp_{\min},\dots tp_{\max}\} \qquad \forall o \in T \quad (20)$$

$$r_o^m = 1 + (tp_o^m - tp_{init})\Delta r_o \qquad \forall o \in T \quad (21)$$

$$V_e^m = 1 \qquad \forall e \in E \quad (22)$$

$$\theta_e^m = 0 \qquad \forall e \in E \quad (23)$$

$$V_{\min} \le V_b^m \le V_{\max} \qquad \forall b \in N \quad (24)$$

$$\bar{S}_{sn\{l\}}^m = \bar{Y}_l^*[(V_{sn\{l\}}^m)^2 - (\bar{V}_{sn\{l\}}^m)(\bar{V}_{m\{l\}}^m)^*] \qquad \forall l \in L-C \quad (25)$$

$$\bar{S}_{m\{l\}}^m = \bar{Y}_l^*[(V_{m\{l\}}^m)^2 - (\bar{V}_{sn\{l\}}^m)^*(\bar{V}_{m\{l\}}^m)] \qquad \forall l \in L-C \quad (26)$$

$$\bar{S}_{sn\{c\}}^m = \bar{Y}_{sn\{c\}}^*(V_{sn\{c\}}^m)^2 - km_{a1\{c\}}^m e^{-j\phi_{1\{c\}}^m}\bar{Y}_{sn\{c\}}^* E_{dc}\bar{V}_{sn\{c\}}^m \qquad \forall c \in C \quad (27)$$

$$\bar{S}_{m\{c\}}^m = \bar{Y}_{m\{c\}}^*(V_{m\{c\}}^m)^2 - km_{a2\{c\}}^m e^{-j\phi_{2\{c\}}^m}\bar{Y}_{m\{c\}}^* E_{dc}\bar{V}_{m\{c\}}^m \qquad \forall c \in C \quad (28)$$

$$\mathrm{Re}\{\bar{S}_{01\{c\}}^m\} + \mathrm{Re}\{\bar{S}_{02\{c\}}^m\} = 0 \qquad \forall c \in C \quad (29)$$

$$Y_{sn\{c\}}^2[(V_{sn\{c\}}^m)^2 + k^2(m_{a1\{c\}}^m)^2 E_{dc}^2 - 2km_{a1\{c\}}^m E_{dc}V_{sn\{c\}}^m\cos(\theta_{sn\{c\}}^m - \phi_{1\{c\}}^m)] \le I_{rate}^2 \qquad \forall c \in C \quad (30)$$

$$Y_{m\{c\}}^2[(V_{m\{c\}}^m)^2 + k^2(m_{a2\{c\}}^m)^2 E_{dc}^2 - 2km_{a2\{c\}}^m E_{dc}V_{m\{c\}}^m\cos(\theta_{m\{c\}}^m - \phi_{2\{c\}}^m)] \le s_c I_{rate}^2 \qquad \forall c \in C \quad (31)$$

$$\sum_{\pi_k^R\in\Pi^R}\pi_k^R(s_c^m) \ge 1 \qquad \forall R \quad (32)$$

$$\sum_{c\in C}s_c^m = \sum_{c\in C}s_c^0 \qquad (33)$$

$$(S_{sn,m\{l\}}^m)^2 \le S_{\max}^2 \qquad \forall l \in L \quad (34)$$

$$P_{e\{b\}}^m + jQ_{e\{b\}}^m + P_{g\{b\}}^m = \omega_d^m(P_{d\{b\}} + jQ_{d\{b\}}) + \sum_{l\in L|sn=b}\bar{S}_{sn\{l\}}^m + \sum_{l\in L|m=b}\bar{S}_{m\{l\}}^m \quad (35)$$

The objective function is given by (16) to minimise the DG curtailment and system losses in terms of operational cost that is aggregated with cost coefficients, c_1 and c_2 at 97.46 $MW^{-2}h^{-1}$ and 0.8959 $MW^{-1}h^{-1}$, respectively. The active and reactive power limits that flow through the primary substation transformer are given by (17) and (18). The operating boundary of DG in (19) is used to correlate with the available resources. Equations (20) – (23) give constraints on the tap changer ratio and voltage magnitude/angle for the slack bus (grid supply point).The statutory voltage limits for all buses are defined in (24). The complex power flow equations for normal lines are expressed in (25) and (26). The power flow equations in (27) and (28) are used for the lines installed with BTB-VSC that must operate within the converter limits in (29) – (31). A binary variable, s_c that is imposed in (31) must fulfill constraints (32) and (33) to enforce radiality in the network reconfiguration. The thermal limits of lines as given in (34) must be obeyed at all the times. Constraint (35) is used to ensure power balance at each bus. It should be noted that the RCSs model uses the nodal power flows in (25) and (26) multiplied with the binary variable, s_c to replace (27) and (28) without the constraints in (29) – (31).

APPENDIX B:
PARAMETER SETTINGS

The parameter settings of control devices, demand and DG profiles are given in the following tables:

TABLE IV: PARAMETER SETTINGS OF CONTROL DEVICES

Control devices	Placement (Buses)	Parameter settings
OLTC transformer	1 (GSP)	$tp_{min} = 1$, $tp_{max} = 13$, $tp_{init} = 7$, $\Delta r_o = 0.01$ p.u.
DG units	6, 7, 13, 18, 28, 33	Power capacity = 1 MW
BTB-VSCs	7, 9, 12, 18, 20, 21, 22, 23, 27	$I_{rate} = 240$ A, $x_{cr} = 16$ Ω, $E_{dc} = 25.32$ kV

TABLE V: DEMAND AND DG PROFILES

m	ω_d	P_{ava}	*m*	ω_d	P_{ava}	*m*	ω_d	P_{ava}
1	0.61	0	9	0.61	0.32	17	0.93	0.28
2	0.49	0	10	0.84	0.57	18	0.86	0.02
3	0.47	0	11	0.93	0.84	19	0.88	0.04
4	0.46	0	12	0.99	1	20	0.91	0
5	0.42	0	13	1	0.99	21	0.86	0
6	0.44	0	14	0.92	0.87	22	0.81	0
7	0.43	0	15	0.96	0.76	23	0.70	0
8	0.40	0.11	16	0.96	0.53	24	0.65	0

Note: All values are presented in per unit (p.u.)